Ti|Ir–Sn–Sb oxide anode: Service life and role of the acid sites content during water oxidation to hydroxyl radicals

Zaira G. Aguilar [a], Oscar Coreño [b], Mercedes Salazar [c], Ignasi Sirés [d], Enric Brillas [d], José L. Nava [a,*]

[a] *Departamento de Ingeniería Geomática e Hidráulica, Universidad de Guanajuato, Av. Juárez 77, Zona Centro, C.P 36000 Guanajuato, Guanajuato, Mexico*

[b] *Departamento de Ingeniería Civil, Universidad de Guanajuato, Av. Juárez 77, Zona Centro, C.P 36000 Guanajuato, Guanajuato, Mexico*

[c] *Departamento de Ingeniería en Minas, Metalurgía y Geología, Universidad de Guanajuato, ExHacienda San Matías S/N, C.P. 36020, Guanajuato, Guanajuato, Mexico*

[d] *Laboratori d'Electroquímica dels Materials i del Medi Ambient, Departament de Química Física, Facultat de Química, Universitat de Barcelona, Martí i Franquès 1-11, 08028 Barcelona, Spain*

* Corresponding author: E-mail address: jlnm@ugto.mx (J.L. Nava)

Abstract

This work describes the preparation of four Ti|Ir–Sn–Sb oxide anodes by the Pechini method under different conditions and the evaluation of their service life, envisaging a future application in electrochemical advanced oxidation processes for water treatment. This was estimated by means of accelerated life tests (1 A cm^{-2}, 1 M $HClO_4$), which highlighted the dependence of durability on the Ir and Sn content in the mixed metal oxide (MMO) as well as on the required heat treatment time for its preparation. The best MMO anode reached up to 351 h of service life under such extreme conditions. SEM-EDS and XRD analyses were performed before and after the accelerated life tests, evidencing that the failure of the MMO coatings occurred by detachment from the titanium substrate, thus losing the anode electroactivity. Great amounts of acid sites in the range 0.21-0.26 meq g^{-1} were determined on the MMO surfaces by Boehm titrations. From the apparent rate constants determined for the decay of *N*,*N*-dimethyl-4-nitrosoaniline used as spin trap, before and after acid sites neutralization, a higher activity of adsorbed hydroxyl radicals at the MMO surface cannot be correlated with a greater amount of acid sites. The results obtained suggest that other active sites affect the formation of such radicals from water discharge.

Keywords: Accelerated life tests; Mixed metal oxide anode; Acid site; Hydroxyl radical; Anodic oxidation.

1. Introduction

Dimensionally stable anodes (DSA®) were developed by Beer in the late 1960s. Although their primary application has been recognized in the chlor-alkali industry [1], they are widely used for the degradation of persistent organic pollutants (POPs) in water [2-15]. These works highlighted that mixed metal oxides (MMO) supported on either titanium or niobium substrates represent one of the most important categories of electrocatalysts [4-11,13-15]. In recent years, electrochemical advanced oxidation processes (EAOPs) using pure metal anodes like Pt, metal oxides (MO) such as PtO, IrO_2, RuO_2, SnO_2 and PbO_2, and MMO like SnO_2-Sb_2O_5, TiO_2-SnO_2 and IrO_2-SnO_2-Sb_2O_5, among others, have been investigated in detail for environmental preservation [13,16]. The high oxidation power of these anodes has been confirmed upon degradation of all kinds of POPs in synthetic and real water effluents.

The anode material plays a fundamental role for the development of effective electro-oxidation (EO) methods, being necessary to prevent typical surface failure and fouling that cause the anode deactivation [17,18]. At present, boron-doped diamond (BDD) anode is considered the best electrode for the EO of POPs [13,16]. Its success is attributed to the large production of physisorbed hydroxyl radicals (BDD($^{\bullet}$OH)) via water oxidation, leading to the complete mineralization of the organic matter in most cases. However, the high cost of BDD anodes has limited its use to small devices. Hence, the design and synthesis of much less expensive MMO anodes is now attracting a lot of attention [4,6-10,14,15]. The preparation of an ideal MMO electrode must guarantee its high oxidation ability, chemical and mechanical stability based on an adequate service life, and low cost. Worth mentioning, the use of MMO for POPs degradation has only been performed at small scale due to limitations from short service life and passivation, which has impeded its industrial application so far [3,12,19].

The MMO anodes are composed of a metal substrate coated with an electrocatalytic layer. Ti, Ta, Zr, W, Nb and Bi are typical substrates, being Ti the most common, whereas Pt, Ir, Ru, Sn, Ir and Ru are used as electrocatalysts, either pure or as metal oxides. Other metal oxides such as TiO_2, Ta_2O_5, ZrO_2, Nb_2O_5 and SnO_2 are used as dispersing or stabilizing agents, and Sb is often added as a doping mediator [20]. RuO_2-based MO anodes are suitable to evolve Cl_2, but they are stable only at alkaline conditions [20], with modest service life under acidic conditions even when a stabilizer is used [21]. In contrast, IrO_2-based anodes are typically chosen as optimum electrocatalysts to promote the O_2 evolution reaction, being stable in acid media [20], with moderate service life in alkaline media [22]. SnO_2 possesses interesting properties to produce physisorbed hydroxyl radicals (M($^{\bullet}$OH)) but its great drawback is the short service life [3]. MMO electrodes like IrO_2-SnO_2-Sb_2O_5 tend to increase the stability and durability, and show higher conductivity [20]. Furthermore, the IrO_2 interlayer enhances the generation of physisorbed hydroxyl radicals (M($^{\bullet}$OH)). Thus, IrO_2 acts as catalyst, SnO_2 behaves as dispersing agent and catalyst, while Sb_2O_5 is a dopant.

The performance of the MO and MMO electrodes depends on: (i) the preparation method of the ink to be deposited onto the substrate (sol–gel or polymeric precursor method), (ii) the coating method (immersion, painting, electrophoresis) [23], (iii) the thermal treatment to obtain the MO or MMO crystallographic phases, and (iv) the substrate pre-treatment [9]. In earlier articles, we demonstrated the good performance of a Ti|Ir-Sn–Sb oxide anode for the EO treatment of dyes like Methyl Orange [9], Indigo [11] and Acid Yellow 36 [15]. The oxidation of water to adsorbed M($^{\bullet}$OH) on the Ti|Ir-Sn–Sb oxide surface may be carried out according to a mechanism that relies on the adsorption of the water molecule on the acid sites of MMO (reaction (1)), which arise from the acid nature of the Ir-Sn-Sb oxides. This is followed by water

discharge via reaction (2). Therefore, the determination of the surface acid sites content is necessary.

$$H_2O + M \rightarrow M(H_2O) \quad (1)$$

$$M(H_2O) \rightarrow M(^{\bullet}OH) + H^+ + e^- \quad (2)$$

The evidence of M($^{\bullet}$OH) production at Ti|Ir-Sn–Sb oxide anode was demonstrated in previous communications of our group, using either spin-trapping with *N*,*N*-dimethyl-4-nitrosoaniline (RNO) [3,10] or by electron paramagnetic resonance (EPR) [15]. However, the characterization of the acid sites has not been reported yet.

The aim of this article is the preparation of Ti|Ir-Sn-Sb oxide anodes by the polymeric precursor method (Pechini method), which show several advantages [10], and the evaluation of their service life, as well as to ascertain the role of the acid sites in the formation of M($^{\bullet}$OH) from water discharge. The service life was estimated using accelerated life tests, in strong acidic medium under galvanostatic conditions. The influence of the Ir, Sn an Sb molar percentage on service life was also addressed. The acid sites content was determined by the Boehm titration method, which consists in neutralizing the acid sites with a carbonate or hydroxide [24,25]. Scanning electron microscopy (SEM) and X-ray diffraction (XRD) were used to examine the morphological and structural changes of the coating.

2. Experimental

2.1. Chemicals

All solutions were prepared with deionized water. The chemicals for the MMO preparation were $H_2IrCl_6 \times H_2O$, $SnCl_4$, $SbCl_3$, citric acid and ethylene glycol of analytical grade purchased from Sigma-Aldrich. RNO and phosphate buffer used for the M($^{\bullet}$OH) detection were of

analytical grade supplied by Sigma-Aldrich. Perchloric acid used for accelerated life tests and other chemicals employed for the pre-treatment of the Ti surface were of reagent grade also provided by Sigma-Aldrich.

2.2. Preparation of the MMO electrodes

The Ti plates were pre-treated by consecutive immersion in concentrated HCl at 70 °C for 1 h and concentrated HNO_3 at room temperature for 20 min. Then, the plates were rinsed with distilled water and dried at room temperature. This pre-treatment served to increase the surface roughness and improve the coating adhesion. Each plate was 4 cm long, 0.5 cm wide and 0.1 cm thick.

The polymeric precursor solution to perform the Pechini method was prepared by mixing citric acid (CA) and ethylene glycol (EG) at 60-70 °C, according to the molar contents summarized in Table 1. The metallic precursors ($H_2IrCl_6 \times H_2O$, $SnCl_4$ and $SbCl_3$) were added to the mixture (see Table 1), maintaining the temperature at 60-70 °C for 30 min. The resulting solutions were used to coat the pre-treated Ti substrates on both sides using a brush. To obtain electrodes E1 and E3, the coated Ti was heated at 115 °C for 15 min in a furnace to induce the polymerization of the precursor. The overall procedure was repeated until forming 32 layers and, finally, the electrodes were heated at 550 °C for 1 h. To obtain electrodes E2 and E4, the heating after the application of the solution onto the pre-treated Ti substrate was made at 550 °C for 10 min, and the overall procedure was repeated to form 32 layers. A final heating at 550 °C was performed for 1 h. The temperature was controlled to avoid the formation of TiO_2, which occurs at 600 °C, because it would cause passivation [26].

2.3. Surface characterization of the electrodes

The morphological characteristics and distribution of metal oxides of the Ti|Ir-Sn–Sb oxide electrodes were evaluated by SEM, using a Carl Zeiss EVO HD15 scanning electron microscope, coupled with an integrated energy dispersive X-ray detector. The crystal structure of the MMO was analyzed by XRD using a Rigaku Ultima IV diffractometer. The diffraction patterns were measured in the 2θ range from 20º to 70°, using Cu $K\alpha_1$ λ=1.5418 Å.

2.4. Detection of generated hydroxyl radicals

RNO was employed as a spin trap for the detection of low concentrations of M(•OH) formed at the MMO surfaces. This technique is based on the analysis of the solution bleaching, which is confirmed from the absorbance decay at λ_{max} = 440 nm [3,10,17]. More details about its effectiveness are reported in previous work [3,10,27]. The absorption spectra of RNO were recorded using a Perkin Elmer Lambda UV/Vis spectrophotometer coupled to an anode half-cell for the *in-situ* detection of M(•OH). A divided three-electrode cell was employed in order to avoid cathodic interferences during the detection process. Two quartz cells typically used in UV/Vis spectrophotometry were utilized to construct the two half cells, which were connected through a saline bridge of Pyrex glass (containing phosphate buffer) and with a Pt wire welded at each extreme. An MMO anode of 0.66 cm^2 area in contact with 3 mL of anolyte (5.2×10^{-5} M RNO in phosphate buffer at pH = 7) and a carbon rod cathode in contact with the same volume of catholyte (phosphate buffer at pH = 7)) were used. The reference electrode was an Ag/AgCl (saturated KCl) electrode immersed in a Luggin capillary, which was carefully inserted into the anodic half-cell. The microelectrolysis tests were performed at 25 ºC using a BioLogic® SP 150 potentiostat-galvanostat running with EC-Lab® software. All the electrode potentials reported in this work are referred to the standard hydrogen electrode (SHE). The oxidation of water was performed at constant anode potential of 1.3 V|SHE for 2 h, carrying

146 out the *in-situ* monitoring of RNO bleaching from starting yellow solution. Note that the
147 selection of such anode potential was made on the basis of previous optimization work [10].
148 The absorption spectra of RNO were recorded in the wavelength range between 375 and 515
149 nm, every 10 min during the 2-h trials.

150 *2.5. Accelerated life tests*

151 The accelerated life test method allowed estimating the service life of the anodes. This
152 procedure was carried out by applying a constant current density (j) of 1 A cm^{-2} to the cell
153 containing 1 M $HClO_4$ at 25 ºC, maintained with a recirculation water bath. A typical undivided
154 three-electrode cell made of Pyrex glass with double jacket containing 70 mL of solution was
155 employed. An MMO of 1 cm^2 and a graphite rod with the same area were used as the anode
156 and cathode, respectively, whereas an Ag/AgCl (saturated KCl) was utilized as the reference
157 electrode. The anode potential was plotted against the electrolysis time until an exponential
158 increase of the signal was observed and thus, the time needed for this drastic change was
159 considered as the service life of the MMO anode. The dramatic increase of the anode potential
160 informs about the anode deactivation due to coating failure. Note that this type of test is usually
161 made in strongly acidic media to mimic chemically corrosive environments [19,20].

162 *2.6. Determination of the acid sites content on the MMO anode*

163 The determination of the surface acid sites content was carried out by the Boehm titration
164 [24,25]. To do this, about 0.40 g of electrode material was added to 40 mL of a 0.01 M NaOH
165 solution and maintained under vigorous stirring for 24 h. After that, the resulting solution was
166 titrated with 0.1 M HCl, under magnetic stirring. The pH of the suspension was measured in
167 continuous until reaching the equilibrium. This allowed identifying the milliequivalents of acid
168 sites content per gram of MMO anode (meq g^{-1}) present on its surface. The relationship between

the acid sites content and the rate of M(•OH) production (known from RNO analyses) from combined reactions (1) and (2) was assessed.

3. Results and discussion

3.1. SEM-EDS and XRD characterization

Fig. 1 shows the SEM micrographs obtained for the surfaces of the four MMO electrodes prepared, namely E1, E2, E3 and E4. The chemical composition, revealing the metal ratio in each coating, was analyzed semi-quantitatively by EDS, as collected in Table 2. The SEM image of electrode E1 shows an irregular surface with high roughness, where some small lumps can be observed. Conversely, micrographs of electrodes E2, E3 and E4 highlight much more flat, regular surfaces with good-looking coatings, as expected from a better integration of Ir, Sn and Sb oxides onto the Ti substrate. Electrode E2 presents the less rough surface, which is attributed to the highest content of Ir and Sn, accounting for up to 24.89 at.%. Note that, in particular, Sn was the most abundant metallic element on E2 surface, reaching 21.02 at.%, whereas Ti was detected at the lowest concentration, i.e., 0.75 at.%. The large accumulation of Sn in E2 is apparently surprising, since its molar ratio in the precursor solution was the same as that used for E1, and much lower than those employed for E3 and E4 (Table 1). This means that the much smaller amounts of polymeric precursors, CA and EG, favor the deposition of Sn. In addition, such low amounts of organic compounds enhance the homogeneity of the E2 coating. The sum of Ir and Sn before the tests in the E1, E3 and E4 electrodes was smaller, with values of 20.06, 8.25 and 17.29 at.%, respectively. Therefore, it seems that a higher Sn content is associated to more homogenous and flat coatings, whereas excessively high Ir contents tend to promote irregularities on the surface (Table 2, anode E1).

191 The X-ray diffraction patterns of the E1, E2, E3 and E4 coatings are presented in Fig. 2.
192 Peaks that can be assigned to Ti, Ir, Sb, Sn, Sb_2O_5, $Sb_{31}Ti_{43.35}$ and SnO_2 phases were found in
193 the four electrodes, highlighting that neither IrO_x nor TiO_x ones were identified. In all these
194 XRD patterns, a broad peak typically associated to an amorphous phase can be observed
195 between 32° and 42°. Other weak peaks at 55.0°, 56.5°, 61.5° and 66.5° could not be assigned
196 to any phase. Since IrO_x was not be detected in the diffractograms, it is reasonable to assign the
197 latter XRD peaks to a highly intermixed Ir-Sn-Sb oxide that formed a solid solution. This might
198 be explained by the kind of synthesis employed, which included a thermal treatment that
199 promotes the solid state diffusion of all metals to form the final MMO [15].

200 *3.2. Influence of acid sites content on the formation of adsorbed hydroxyl radicals*

201 Table 3 summarizes the acid sites content found for the four electrodes prepared, which
202 reached high values varying from 0.21 to 0.26 meq g^{-1}. In order to elucidate whether these acid
203 sites play a fundamental role in the formation of hydroxyl radicals onto the surface of the MMO
204 anodes, the kinetics of RNO removal upon EO treatment was studied by carrying out several
205 microelectrolyses, in the presence and absence of acid sites. UV/Vis spectra of the solutions
206 were recorded and the maximum absorbance values were determined at λ = 440 nm.

207 Fig. 3 depicts the time course of the absorption spectra of RNO with electrolysis time for
208 the four anodes in the presence of their natural acid sites. A regular decay of the RNO
209 absorbance until 120 min of electrolysis can be observed for all the electrodes, thereby
210 confirming its reaction with adsorbed M($^{\bullet}$OH) in all cases. A similar set of trials was performed
211 after the neutralization of the acid sites onto the MMO electrodes (not shown). Fig. 4a and b
212 shows the decay of the RNO concentration as a function of time in the presence and absence of
213 acid sites, respectively. The corresponding inset panels show the semi-logarithmic plots of these

curves and evidence the good fit. Therefore, the concentration decay follows a pseudo-first-order reaction kinetics in both sets of experiments, which means that a constant concentration of M(•OH) is formed during the EO treatments with these types of anodes, either in the absence or presence of acid sites. This is then a relevant finding, since it suggests that M(•OH) production from water oxidation is not controlled by the amount of acid sites. Table 3 collects the apparent rate constants in the presence (k_{app}) and absence (k_{app}*) of acid sites, as determined from the slopes of the linear correlations shown in the insets of Fig. 4a and b. These data show that the kinetics of M(•OH) formation is not proportional to the number of acid sites. For example, the concentration of such sites on the MMO electrodes increased in the order: E2 < E3 < E4 < E1, whereas k_{app} rose as E4 ≤ E1 < E3 < E2. In the absence of the acid sites, k_{app}* slightly decreased as compared to k_{app}, growing in the order E1< E4 < E3 < E2, that is, inversely to the initial concentration of acid sites. Overall, our results suggest that other kinds of active sites seem to catalyze the M(•OH) production.

3.3 Accelerated life tests performed on the MMO electrodes

The results obtained for the accelerated life tests of the four electrodes used as anodes are presented in Fig. 5. As can be seen, the anode potential versus electrolysis time plots were recorded until a drastic potential rise appeared, being this time assumed as the service life of each MMO anode. The service life of the anodes tested decreased according to the following sequence: E2 >> E4 > E1 > E3. It is particularly remarkable the long service life of electrode E2, as long as 351 h, in contrast to the very short ones of E1 (23 h) and E3 (13 h). Although the service life of 37 h of the E4 electrode was superior to those of the two latter ones, it underwent a progressive passivation from the beginning of the accelerated life test, suggesting that the E4 electrode was the less stable MMO of the anodes synthesized. On the other hand, the good

237 performance of E2 can be related to the regular and uniform surface coverage shown in Fig. 1,
238 which is in turn associated to the large presence of SnO_2 (Table 2). Furthermore, the higher
239 temperature used for E2 and E4 electrodes (consecutive cycles at 550 ºC) also seems to
240 contribute favorably to their larger stability as a result of a better adhesion of the MMO coating
241 on the Ti substrate.

242 The metal content in the coatings after the accelerated life tests is also listed in Table 2.
243 These data evidence a high increase in the percentage of Ti, along with a notable decrease of
244 the percentages of Ir, Sn and Sb, as compared to those measured in the raw electrodes. This
245 behavior confirms that the coatings were detached from the titanium surface during the
246 accelerated life tests. Worth mentioning, when using these anodes for the EO treatment of
247 POPs, the formation of some by-products may lead to the appearance of metal complexes,
248 which could cause a quicker destabilization of the electrodes. Then, the accelerated life test
249 method only allows the estimation of the service life of the MMO anodes.

250 Finally, just as an example, if we consider the use of the E2 anode in an EO at a j = 10 mA
251 cm^{-2} to mineralize POPs, assuming the absence of polymer film formation on the E2 anode
252 surface during the electrolysis, one can infer that this MMO anode would have a service life as
253 long as 1460 days (about 4 years).

254

4. Conclusions

Ti plates were successfully coated with Ir, Sn and Sb oxides by the polymeric precursor method (Pechini method). SEM-EDS and XRD corroborated that the synthesized electrodes were mainly composed of a mixture of Ir-Sn-Sb oxides. The analysis of service life of four different anodes, estimated from accelerated life tests at 1 A cm^{-2}, highlighted that a high Sn content and high heating temperature are crucial parameters. The best MMO anode reached up to 351 h of service life. EDS analyses proved that the coatings were detached from the substrate during the accelerated life tests. The acid sites content on the surface of the anodes varies between 0.21-0.26 meq g^{-1}, but it cannot be correlated with a larger or poorer production of M($^{\bullet}$OH) from water discharge.

Acknowledgements

Financial support from projects 240522 (CONACYT, Mexico) and 869/2016 (University of Guanajuato, Mexico) is acknowledged. The authors also thank financial support under project CTQ2016-78616-R (AIE/FEDER, EU). The help from Dr. Raul Miranda and Daniela Moncada from LICAMM-UG Laboratory for SEM and XRD analysis is acknowledged. Z.G. Aguilar is grateful to CONACYT for the PhD scholarship No. 421053 granted.

References

[1] S. Trasatti, Electrocatalysis: Understanding the success of DSA®, Electrochim. Acta 45 (2000) 2377-2385.

[2] R. Kötz, S. Stucki, B. Carcer, Electrochemical waste water treatment using high overvoltage anodes. Part I: Physical and electrochemical properties of SnO_2 anodes, J. Appl. Electrochem. 21 (1991) 14-20.

[3] C. Comninellis, Electrocatalysis in the electrochemical conversion/combustion of organic pollutants for wastewater treatment, Electrochim. Acta. 39 (1994) 1857-1862.

[4] C.L. Zanta, P.A. Michaud, C. Comninellis, A.R. Andrade, J.F.C. Boodts, Electrochemical oxidation of *p*-chlorophenol on SnO_2-Sb_2O_5 based anodes for wastewater treatment, J. Appl. Electrochem. 33 (2003) 1211-1215.

[5] K.L. Meaney, S. Omanovic, $Sn_{0.86}$–$Sb_{0.03}$–$Mn_{0.10}$–$Pt_{0.01}$-oxide/Ti anode for the electro-oxidation of aqueous organic wastes, Mater. Chem. Phys. 105 (2007) 143-147.

[6] B. Adams, M. Tian, A. Chen, Design and electrochemical study of SnO_2-based mixed oxide electrodes, Electrochim. Acta. 54 (2009) 1491-1498.

[7] X. Yang, R. Zoua, F. Huo, D. Cai, D. Xiao, Preparation and characterization of Ti/SnO_2–Sb_2O_3–Nb_2O_5/PbO_2 thin film as electrode material for the degradation of phenol. J. Hazard. Mater. 164 (2009) 367-373.

[8] S. Song, L. Zhan, Z. He, L. Lin, J. Tu, Z. Zhang, J. Chen, L. Xu, Mechanism of the anodic oxidation of 4-chloro-3-methyl-phenol in aqueous solution using Ti/SnO_2-Sb/PbO_2 electrodes, J. Hazard. Mater. 175 (2010) 614-621.

[9] R. Chaiyont, C. Badoe, C. Ponce de León, J.L. Nava, F.J. Recio, I. Sirés, P. Herrasti, F.C. Walsh, Decolorization of methyl orange dye at IrO_2-SnO_2-Sb_2O_5 coated titanium anodes, Chem. Eng. Technol. 36 (2013) 123-129.

[10] M.I. León, Z.G. Aguilar, J.L. Nava, Electrochemical combustion of indigo at ternary oxide coated titanium anodes, J. Electrochem. Sci. Eng. 4 (2014) 247-258.

297 [11] J.L. Nava, I. Sirés, E. Brillas, Electrochemical incineration of indigo. A comparative
298 study between 2D (plate) and 3D (mesh) BDD anodes fitted into a filter-press reactor,
299 Environ. Sci. Pollut. Res. 21 (2014) 8485-8492.
300 [12] T.E.S. Santos, R.S. Silva, C.C. Jara, K.I.B. Eguiluz, G.R. Salazar-Banda, The influence
301 of the synthesis method of Ti/RuO_2 electrodes on their stability and catalytic activity for
302 electrochemical oxidation of the pesticide carbaryl, Mater. Chem. Phys. 148 (2014) 39-
303 47.
304 [13] I. Sirés, E. Brillas, M.A. Oturan, M.A. Rodrigo, M. Panizza, Electrochemical advanced
305 oxidation processes: today and tomorrow. A review, Environ. Sci. Pollut. Res. 21 (2014)
306 8336-8367.
307 [14] W. Wu, Z.H. Huang, T.T. Lim, Recent development of mixed metal oxide anodes for
308 electrochemical oxidation of organic pollutants in water, Appl. Catal. A: Gen. 480 (2014)
309 58-78.
310 [15] Z.G. Aguilar, E. Brillas, M.M. Salazar, J.L. Nava, I. Sirés, Evidence of Fenton-like
311 reaction with active chlorine during the electrocatalytic oxidation of Acid Yellow 36 azo
312 dye with Ir-Sn-Sb axide anode in the presence of iron ion, Appl. Cat. B: Environ. 206
313 (2017) 44-52.
314 [16] C.A. Martínez-Huitle, M.A. Rodrigo, I. Sirés, O. Scialdone, Single and coupled
315 electrochemical processes and reactors for the abatement of organic water pollutants: A
316 critical review, Chem. Rev. 115 (2015) 13362-13407.
317 [17] C. Comninellis, G.P. Vercesi, Characterization of DSA®–type oxygen evolving
318 electrodes: choice of a coating, J. Appl. Electrochem. 21 (1991) 335-345.

[18] H. Lin, J. Niu, J. Xu, Y. Pan, Electrochemical mineralization of sulfamethoxazole by Ti/SnO_2-Sb/Ce-PbO_2 anode: Kinetics, reaction pathways, and energy cost evolution, Electrochim. Acta. 97 (2013) 167-174.

[19] B. Correa-Lozano, C. Comninellis, A. de Battisti, Service life of Ti/SnO_2-Sb_2O_5 anodes, J. Appl. Electrochem 27 (1997) 970-974.

[20] X. Qin, F. Gao, G. Chen, Effects of the geometry and operating temperature on the stability of Ti/IrO_2-SnO_2-Sb_2O_5 electrodes for O_2 evolution, J. Appl. Electrochem. 40 (2010) 1797-1805.

[21] L. Vázquez-Gómez, S. Ferro, A. De Battisti, Preparation and characterization of RuO_2-IrO_2-SnO_2 ternary mixtures for advanced electrochemical technology, Appl. Catal. B: Environ. 67 (2006) 34-40.

[22] S. Cherevko, S. Geiger, O. Kasian, N. Kulyk, J.P. Grote, A. Savan, B.R. Shrestha, S. Merzlikin, B. Breitbach, A. Ludwig, K.J.J. Mayrhofer, Oxygen and hydrogen evolution reactions on Ru, RuO_2, Ir, and IrO_2 thin film electrodes in acidic and alkaline electrolytes: A comparative study on activity and stability, Catal. Today 262 (2016) 170-180.

[23] R.A. Herrada, A. Medel, F. Manríquez, I. Sirés, E. Bustos, Preparation of IrO_2-Ta_2O_5|Ti electrodes by immersion, painting and electrophoretic deposition for the electrochemical removal of hydrocarbons from water, J. Hazard. Mater. 319 (2016) 102-110.

[24] H.P. Boehm, E. Diehl, W. Heck, R. Sappok, Surface oxides of carbon, Angew. Chem. Int. Ed. 3 (1964) 669-677.

[25] H. Wang, Z. Bian, G. Lu, L. Pang, Z. Zeng, D. Sun, Preparation of multifunctional gas-diffusion electrode and its application to the degrading of chlorinated phenols by electrochemical reducing and oxidizing processes, Appl. Catal. B: Environ. 125 (2012) 449-456.

[26] Y. Xin, L. Xu, J. Wang, X. Li, Effect of sintering temperature on microstructure and electrocatalytic properties of Ti/IrO_2-Ta_2O_5 anodes by Pechini method, Rare Metal Mat. Eng. 39 (2010) 1903-1907.

[27] J. Muff, L.R. Bennedsen, E.G. Søgaard, Study of electrochemical bleaching of *p*-nitrosodimethylaniline and its role as hydroxyl radical probe compound, J. Appl. Electrochem. 41 (2011) 599-607.

Table 1

Molar content of organic chemicals and metals in the polymeric precursor solutions employed for the preparation of different anodes.

Electrode	EG	CA	Ir	Sn	Sb
E1	16	0.12	0.0296	0.0296	0.0004
E2	3.2	0.024	0.0296	0.0296	0.0004
E3	16	12	0.0296	0.2371	0.0296
E4	16	12	0.0296	0.2371	0.0296

Table 2

Atomic percentages of the elements present on the surface of the anodes prepared, namely E1, E2, E3 and E4, as measured by EDS analysis.

Element	E1	E1*	E2	E2*	E3	E3*	E4	E4*
Ti	2.92	38.45	0.75	24.44	2.53	27.18	4.81	24.12
Sn	2.85	0.40	21.02	6.07	5.06	1.55	12.94	0.41
Sb	0.73	0.21	0.77	0.61	2.52	0.81	6.42	0.12
Ir	17.21	0.50	3.87	1.53	3.19	1.40	4.35	0.35
O	76.29	60.44	73.59	67.35	86.70	69.07	71.48	75.00

*After accelerated life test.

360 **Table 3**

361 Acid sites content of the MMO anodes, and apparent rate constants for the decays of the RNO

362 absorbance shown in the semi-logarithmic plots of Fig. 4a,b.

Electrode	Acid sites / meq g^{-1}	k_{app} (s^{-1})	R^2	k_{app}^{*} (s^{-1})	R^2
E_1	0.26	0.0221	0.995	0.0191	0.991
E_2	0.21	0.0265	0.983	0.0230	0.979
E_3	0.22	0.0246	0.994	0.0222	0.989
E_4	0.23	0.0217	0.990	0.0212	0.985

363 *After the acid sites content was neutralized.

364

365 **Figure captions**

366 **Fig. 1.** Scanning electron micrographs of the MMO anodes E1, E2, E3 and E4.

367 **Fig. 2.** XRD patterns of the MMO anodes E1, E2, E3 and E4.

368 **Fig. 3.** Absorption spectra of RNO solutions obtained at 10 min intervals upon 2-h electrolyses
369 using the MMO anodes E1, E2, E3 and E4, with immersed area of 0.66 cm^2. The solutions
370 contained 3 mL of 5.2×10^{-5} M RNO in phosphate buffer solution of pH = 7, at 25 ºC. Anodic
371 potential: 1.3 V|SHE. Measurements were made under quiescent conditions.

372 **Fig. 4.** Change of RNO concentration with electrolysis time using the MMO anodes E1, E2, E3
373 and E4. (a) Curves obtained from absorbance data shown in Fig. 3. (b) Similar curves, obtained
374 after neutralization of acid sites. The inset panels present the corresponding pseudo-first-order
375 kinetic analysis.

376 **Fig. 5.** Service life tests of the MMO anodes E1, E2, E3 and E4. Electrolyses were performed
377 in 1 M HClO, at 1 A cm^{-2} and 25 ºC, using an immersed electrode area of 1 cm^2. Measurements
378 were made under quiescent conditions.
379

380

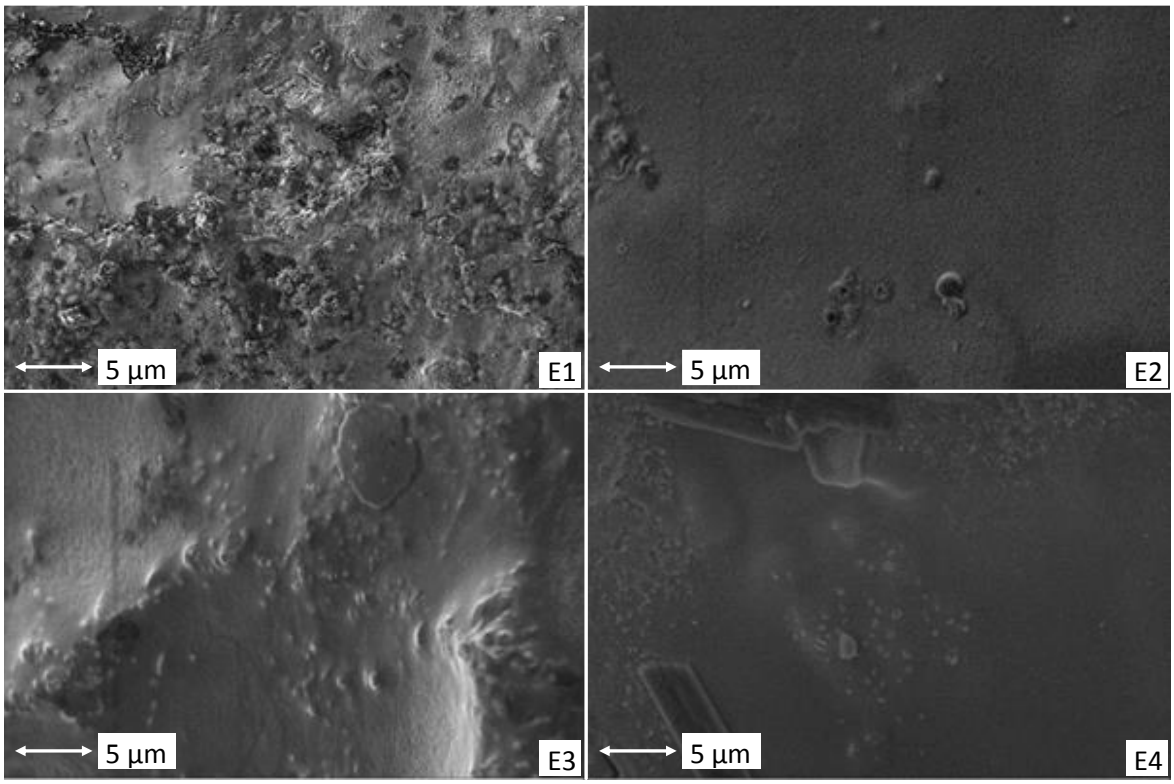

381

382

383

384 **Fig. 1**

385

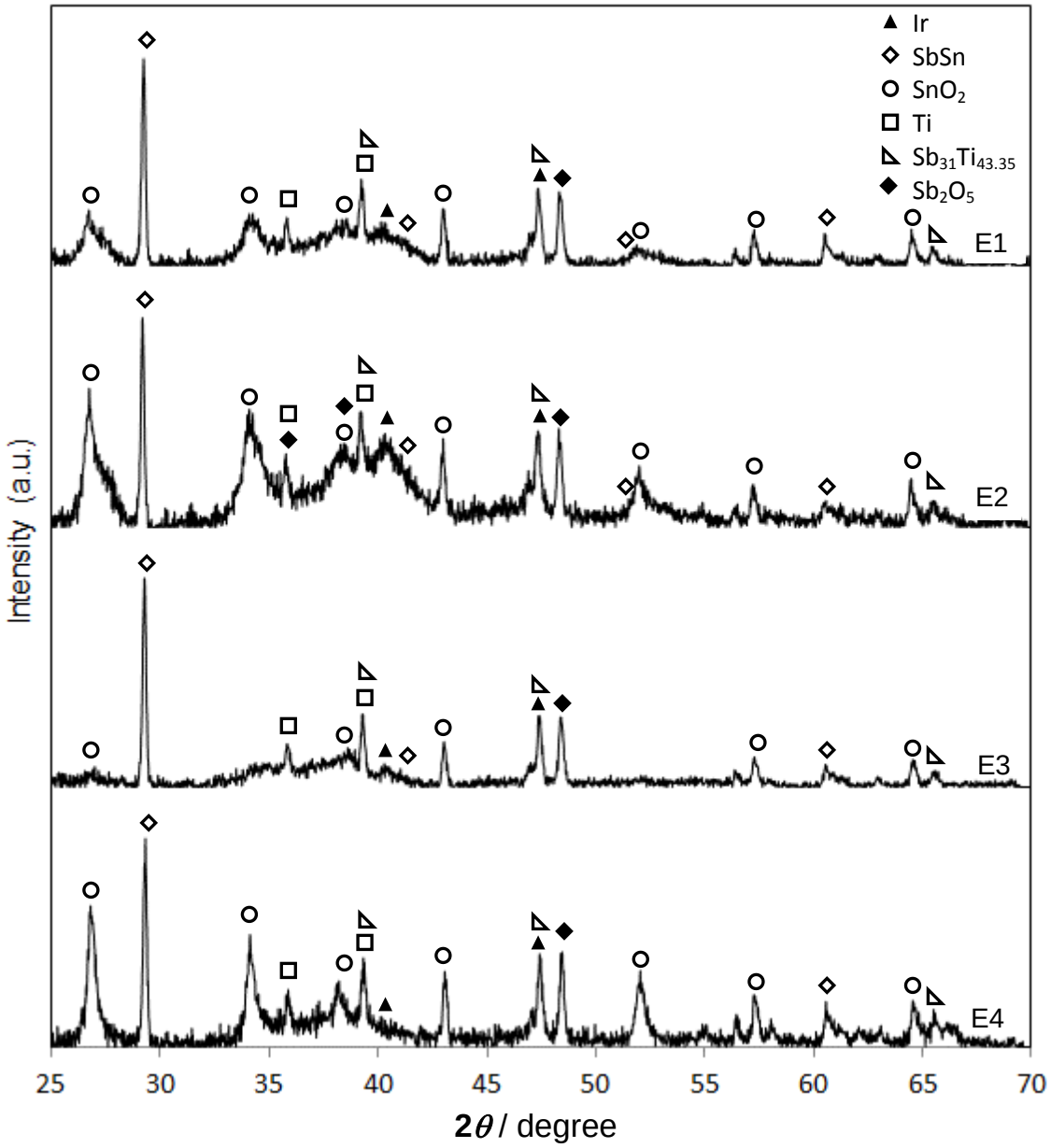

386

387

388

389 **Fig. 2**

390

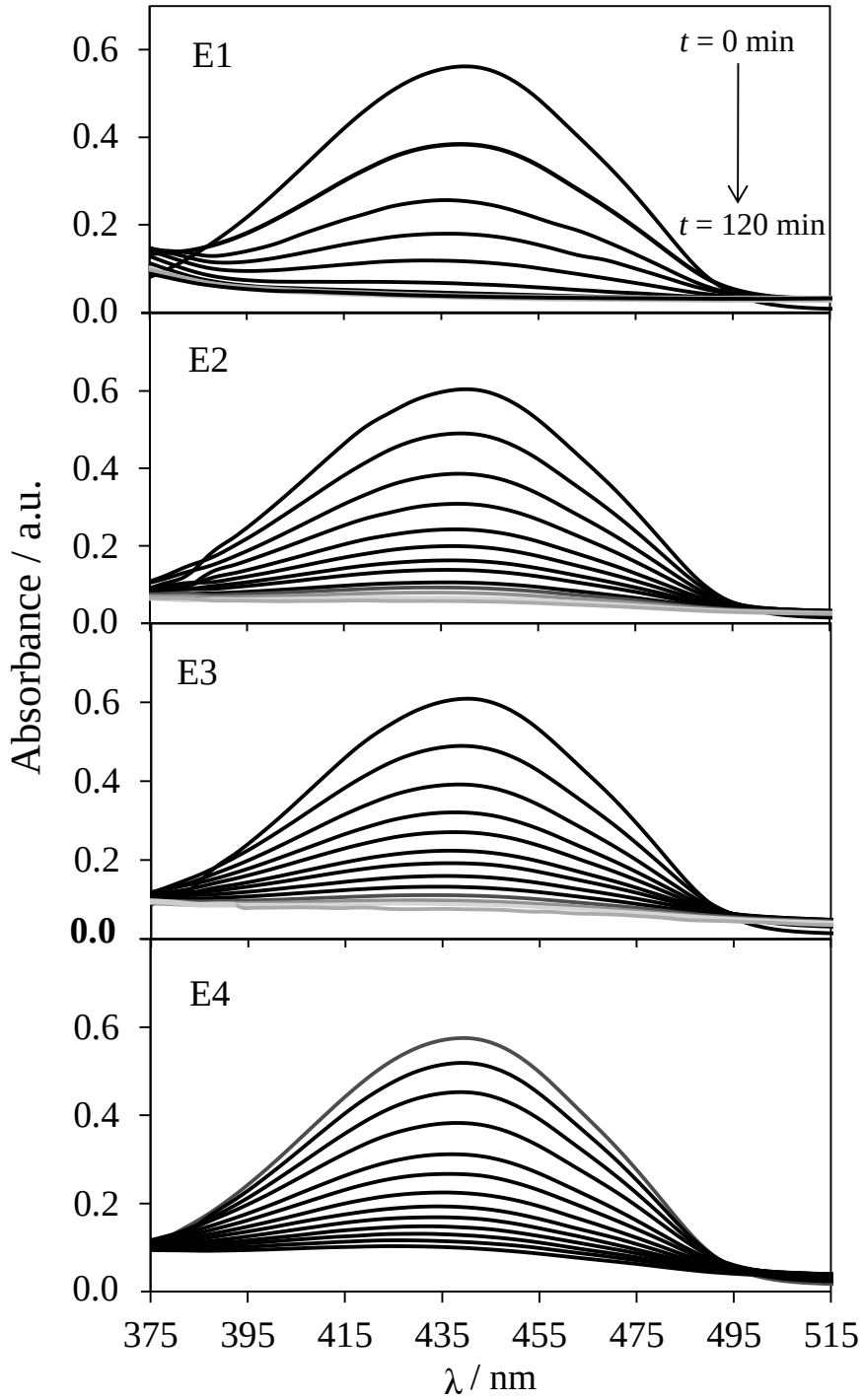
E1
t = 0 min
t = 120 min
E2
E3
E4
Absorbance / a.u.
0.0
0.2
0.4
0.6
375
395
415
435
455
475
495
515
λ / nm

Fig. 3

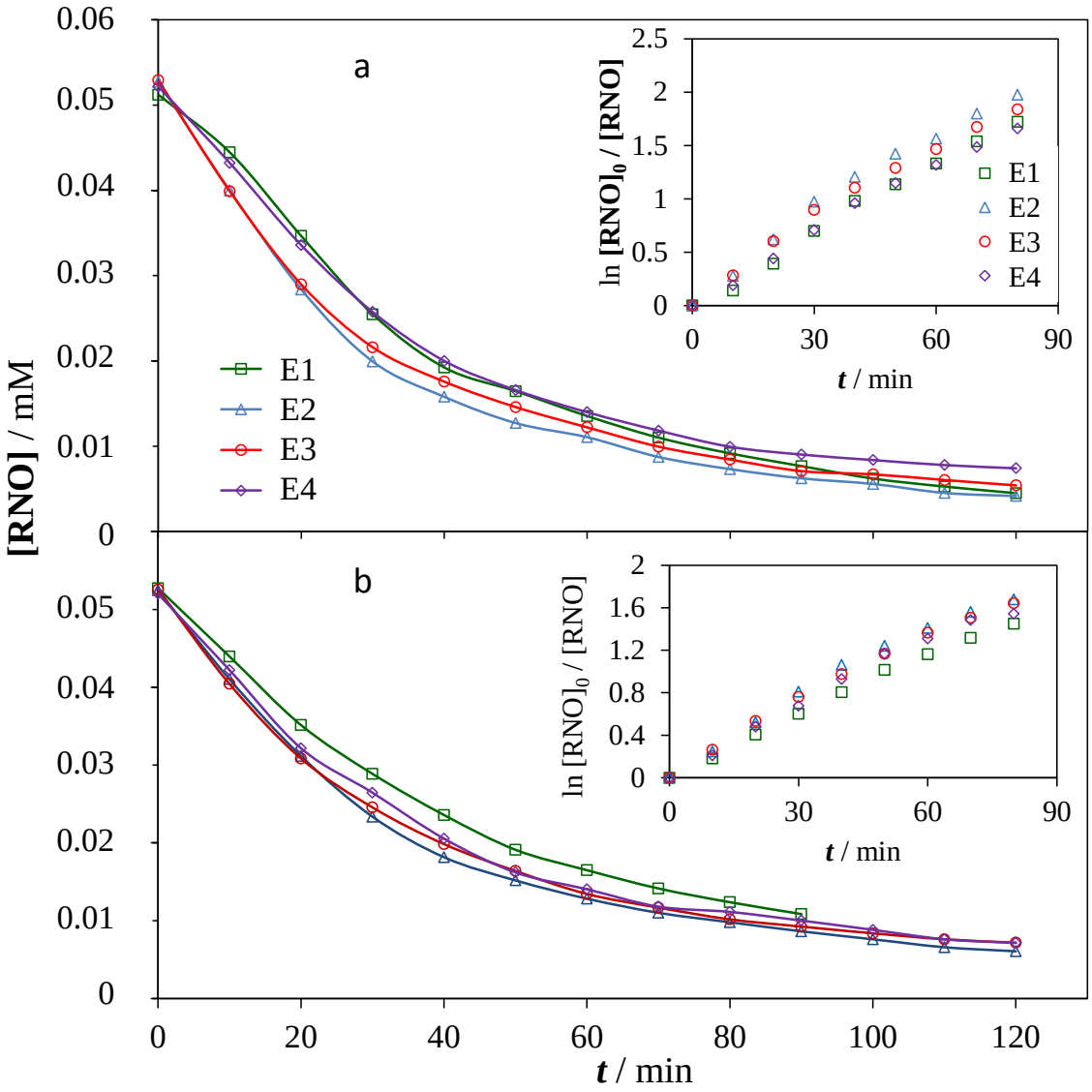
a
b
E1
E2
E3
E4
[RNO] / mM
t / min
ln [RNO]0 / [RNO]
0.06
0.05
0.04
0.03
0.02
0.01
0
20
40
60
80
100
120
90
2.5
2
1.5
1
0.5
1.6
1.2
0.8
0.4

Fig. 4

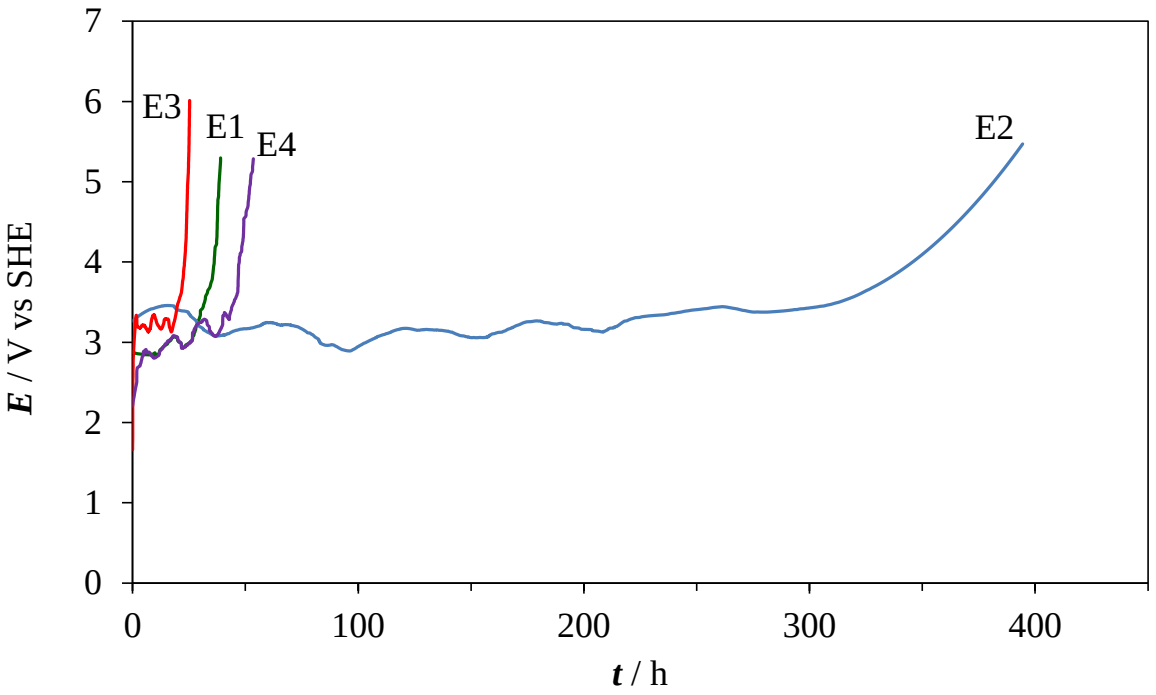

Fig. 5